Climate
of the Past

Open Access

Large spatial variations in coastal ^{14}C reservoir age – a case study from the Baltic Sea

B. C. Lougheed[1], **H. L. Filipsson**[1], **and I. Snowball**[1,2]

[1]Department of Geology, Lund University, Sölvegatan 12, 22362 Lund, Sweden
[2]Department of Earth Sciences – Geophysics, Uppsala University, Villavägen 16, 75236 Uppsala, Sweden

Correspondence to: B. C. Lougheed (bryan.lougheed@geol.lu.se)

Abstract. Coastal locations are highly influenced by input from freshwater river runoff, including sources of terrestrial carbon, which can be expected to modify the ^{14}C reservoir age, or $R(t)$, associated with marine water. In this Baltic Sea case study, pre-bomb museum collection mollusc shells of known calendar age, from 30 locations across a strategic salinity transect of the Baltic Sea, were analysed for ^{14}C, δ^{13}C and δ^{18}O. $R(t)$ was calculated for all 30 locations. Seven locations, of which six are within close proximity of the coast, were found to have relatively higher $R(t)$ values, indicative of hard-water effects. Whenever possible, the *Macoma* genus of mollusc was selected from the museum collections, in order to exclude species specific reservoir age effects as much as possible. When the *Macoma* samples are exclusively considered, and samples from hard-water locations excluded, a statistically significant correlation between *Macoma* $R(t)$ and average salinity is found, indicating a two end-member linear mixing model between ^{14}C$_{marine}$ and ^{14}C$_{runoff}$. A map of Baltic Sea *Macoma* aragonite $R(t)$ for the late 19th and early 20th centuries is produced. Such a map can provide an estimate for contemporary Baltic Sea *Macoma* $R(t)$, although one must exercise caution when applying such estimates back in time or to ^{14}C dates obtained from different sample material. A statistically significant correlation is found between δ^{18}O$_{aragonite}$ and *Macoma* $R(t)$, suggesting that δ^{18}O$_{aragonite}$ can be used to estimate *Macoma* palaeo-$R(t)$, due to the δ^{18}O$_{aragonite}$ signal being dominated by the salinity gradient of the Baltic Sea. A slightly increased correlation can be expected when δ^{18}O$_{aragonite}$ is corrected for temperature fractionation effects. The results of this Baltic Sea case study, which show that $R(t)$ is affected by hydrographic conditions and local carbon inputs, have important consequences for other coastal and estuarine locations, where $R(t)$ is also likely to significantly vary on spatial and temporal bases.

1 Introduction

For the period spanning the past 50 ka, radiocarbon (^{14}C) is the most commonly employed proxy for inferring sample ages and constructing geochronologies. ^{14}C dating has been greatly improved by dendrochronology-based ^{14}C calibration curves (e.g. Stuiver et al., 1998; Reimer et al., 2004), the most recent of which is IntCal09 (Reimer et al., 2009). These calibration curves allow ^{14}C ages to be converted to calibrated ages based on reconstructions of past fluctuations in atmospheric radiocarbon concentration (Δ^{14}C$_{atm}$). ^{14}C is produced in the higher atmosphere and rapidly oxidises to ^{14}CO$_2$, and is mixed quickly and uniformly (< 10 yr) throughout the atmosphere (Damon et al., 1978; Siegenthaler and Oeschger, 1980), meaning that ^{14}C determinations based on terrestrial macrofossils can be accurately calibrated. Atmospheric ^{14}CO$_2$ is absorbed by the oceans and dissolves to H$_2^{14}$CO$_3$, but the relatively slow circulation of the oceans means that this "marine" radiocarbon (^{14}C$_{marine}$), which is incorporated by marine macrofossils, can have an apparent older age (Siegenthaler et al., 1980). The location-specific ^{14}C yr offset from the IntCal09 calibration curve for this older ^{14}C$_{marine}$ is, in the case of a specific calendar age (t), known as the *reservoir age*, or $R(t)$, and knowledge of this age is vital when constructing geochronologies at any given marine location. A marine calibration curve, Marine09 (Reimer et al., 2009), also exists, whereby the offset from

Marine09 is described as ΔR. However, seeing as the Baltic Sea is a shelf sea with strong influence of river runoff, reservoir age is henceforth discussed in this study as $R(t)$, the offset from the IntCal09 calibration curve.

For coastal areas and shelf seas, local hydrographic and environmental factors are especially influential upon $R(t)$. Marine water can contain relatively older ^{14}C than river runoff, the latter of which is equilibrated with relatively younger atmospheric ^{14}C. Coastal areas can be expected to be influenced by both of these sources, as well as other terrestrial sources of carbon of varying age. Such coastal environments exist around the world and have become important study locations due to their potential as high resolution archives of human activity and palaeo-runoff (e.g. Amazon River Delta, Baltic Sea, Black Sea, Gulf of St. Lawrence, Mississippi Delta, Thames Estuary, Yellow River Delta, etc.). Understanding of local reservoir age dynamics is essential when constructing ^{14}C-based geochronologies for these locations. However, there has been only limited research into the modification of coastal reservoir ages by freshwater runoff (e.g. Cage et al., 2006), meaning that investigators in coastal locations often have to apply more general, regional estimates for $R(t)$, often based on reservoir ages in the open ocean, which is far from ideal.

The Baltic Sea is a shelf sea and, with its uniquely large salinity gradient, it provides an ideal location to investigate the interplay between ^{14}C$_{marine}$ and ^{14}C$_{runoff}$. Additionally, the Baltic Sea is heavily influenced by river runoff waters with various carbon inputs, while post-glacial isostatic adjustment has caused changes in water exchange rates with the open ocean. The aim of this study is to investigate a hypothesised relationship between Baltic Sea hydrographic conditions and $R(t)$ by carrying out ^{14}C determinations on pre-bomb mollusc shells with a known calendar age, covering a strategic transect of varying environments, including coastal areas, mid-basin areas, and areas of varying salinity. Additionally, the shells are also analysed for stable isotopes of oxygen and carbon to provide further information on hydrographic conditions.

2 Background

2.1 Hydrographic setting

The Baltic Sea is a continental shelf sea, geographically separated from the global ocean by the sills and islands in the Danish Straits (Fig. 1a). Water exchange between the Baltic Sea and the North Sea is highly restricted and the residence time of Baltic Sea water is currently 25–35 yr (Matthäus and Schinke, 1999). This reduced water exchange is mainly due to the presence of two shallow sills at the entrance to the Baltic Sea at the Danish Straits, the Darss Sill and the Drogden Sill (Fig. 1a). The hydrography of the sea is dominated by river runoff from the large catchment area, which is three times the size of the sea itself. The freshwater surplus of the sea (river runoff + over sea precipitation − sea surface evaporation) amounts to 476 km^3, which is similar to the annual inflowing saline water through the Danish straits of 471 km^3 (Carstensen et al., 2002). This balance has led to the Baltic Sea developing a stratified, positive estuarine circulation with a shallow outflowing mass of fresher water overlying deeper, saline inflowing water. The existence of these two water masses results in a permanent halocline. Both the outflowing and inflowing water masses have innate δ^{18}O$_{water}$ signals and a general ^{18}O end-member mixing relationship is present in the Baltic, whereby the outflowing water is sourced from relatively ^{18}O depleted runoff water (Ehhalt, 1969; Frölich et al., 1988; Punning et al., 1991). Similar end-members have also been found in the case of strontium (Andersson et al., 1992).

2.2 ^{14}C pathways in the Baltic Sea

One cannot at first expect to find a simple end-member mixing model for $R(t)$ that reflects the interaction between inflowing ^{14}C$_{marine}$ and outflowing ^{14}C$_{runoff}$, because the Baltic Sea can be influenced by numerous sources of carbon and radiocarbon (Fig. 2), each exerting a location-specific influence. River input contributes to the terrestrial dissolved organic carbon (tDOC) and dissolved inorganic carbon (DIC) content of the sea waters. tDOC can be sourced from either old or contemporary catchment-specific carbon. DIC in sea water can originate from exchange with atmospheric CO_2 (young ^{14}C age) in runoff water or from marine water with a reservoir of older DIC. Depending on the catchment bedrock, DIC can also be derived from old calcareous bedrock carbon of infinite ^{14}C age, which can significantly increase the measured ^{14}C age of any samples that incorporate such carbon – this is commonly known as the "hard-water effect". Local hard-water DIC can potentially be incorporated in the shells of molluscs and foraminifera when they biomineralise $CaCO_3$, thereby incorporating old carbon of infinite ^{14}C age, which contributes to a significant shell $R(t)$. Autotrophic organisms incorporate DIC during primary production, so carbon with an infinite ^{14}C age can enter the marine food chain in this way. Subsequently, this carbon can be (re)mineralised and recycled between the DIC and marine dissolved organic carbon (mDOC) pools. Large, late summer algal blooms are a common feature in the eutrophic Baltic Sea (Zillén et al., 2008).

As discussed above, dissolved carbon can contribute to the carbon content of macrofossils such as molluscs and foraminifera. In the case of bulk sediment, the source is particulate matter, either organic or inorganic. This particulate matter can either be terrestrial (i.e. from river runoff) or marine (i.e. from primary and secondary productivity) and both contribute to bottom sediment accumulation. The relative contribution of each depends on the location in the Baltic Sea, which is highly influenced by both sources. Particulate
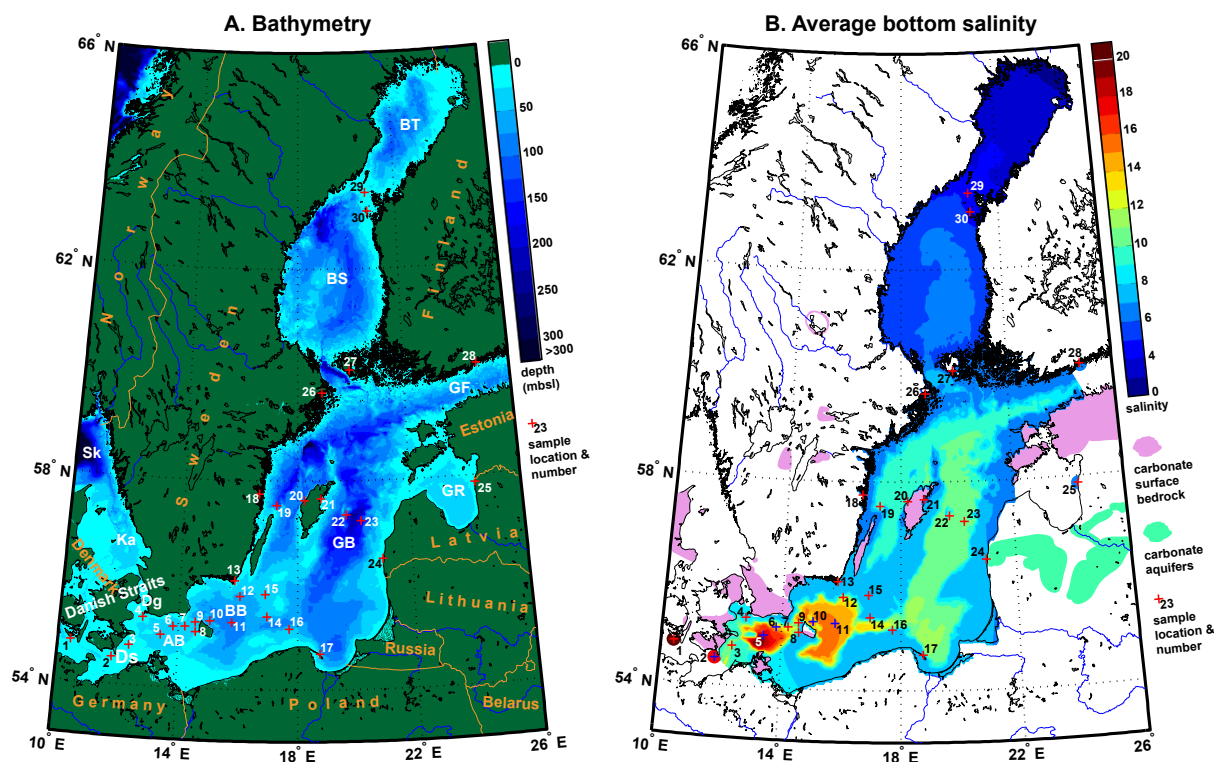
Fig. 1. (A) Baltic Sea bathymetry (IOC et al., 2003) with sample locations shown as crosses with associated sample location numbers in black text. Abbreviated white text denotes the following: Sk = Skagerrak, Ka = Kattegat, Dg = Drogden Sill, Ds = Darss Sill, AB = Arkona Basin, BB = Bornhom Basin, GB = Gotland Basin, GR = Gulf of Riga, GF = Gulf of Finland, BS = Bothnian Sea, and BT = Bothnian Bay. **(B)** Average bottom salinity map for the Baltic Sea, salinity map is for the period 1900–1940 AD from HELCOM (2013). Salinity data for locations 1, 2, 25 and 28 is for the period 1900–1996 AD and from Janssen et al. (1999). Also shown are land areas with carbonate bedrock and aquifers (pink and light green areas, respectively, following Stephens et al., 1994; Kalberg et al., 2007; BGR Hannover et al., 2008).

matter can also remineralise to DIC and DOC. Less contribution of terrestrial particulate matter to bottom sediment can be expected in locations further from the coast. For example, Adolphi (2010) found that the relative contribution of terrestrial input to sediment at the mid-basin Gotland Deep was very low.

It has been common in marine geological literature to simply refer to a general $R(t)$ correction, but in a complex estuarine environment like the Baltic Sea, it is useful to consider such an $R(t)$ correction as comprised of two major components: the first component is the apparent age of the water due to ventilation rates and residence times (i.e. the interplay between the ^{14}C$_{\text{marine}}$ and ^{14}C$_{\text{runoff}}$ end-members). The second component is the influence of old carbon, the so-called "hard-water effect". Both of these two major components can vary independently in the Baltic Sea, both spatially and temporally. Post-glacial isostatic uplift has caused the volume of the sea to decrease by some 47 % since the early Holocene (Meyer and Harff, 2005), with a concomitant 6–8 unit salinity decrease (reported using the dimensionless practical salinity unit – henceforth PSU) (Widerlund and Andersson, 2011). This volumetric change has caused the relative

contribution of ^{14}C$_{\text{marine}}$ to vary. Additionally, precipitation patterns over the Baltic catchment area can change through time, influencing the amount of ^{14}C$_{\text{runoff}}$, which Gustafsson and Westman (2002) estimate could have changed in a range of 15–60 %. Runoff changes can affect not only the circulation and ventilation of Baltic Sea waters, but also the amount of terrestrial carbon (including ^{14}C) that finds its way into the Baltic Sea.

The ^{14}C source pathways play an important role when choosing material for ^{14}C dating. The preferred material for dating is CaCO$_3$ shells of marine micro- and macrofossils such as foraminifera and molluscs, as the ^{14}C source (^{14}CO$_3^{2-}$ ions from ambient seawater DIC) is well constrained. However, the prevalence of anoxic bottom waters in the deeper parts of the Baltic Sea, together with low alkalinity and salinity, means that marine micro- and macrofossils are often scarce in many Baltic Sea sediment cores. Bulk sediment is therefore often used for ^{14}C dating. Bulk sediment is comprised of particulate matter of various terrestrial and marine origins, which may have been resuspended and redeposited multiple times, and the ^{14}C age can depend strongly on the relative contributions of organic and inorganic matter.
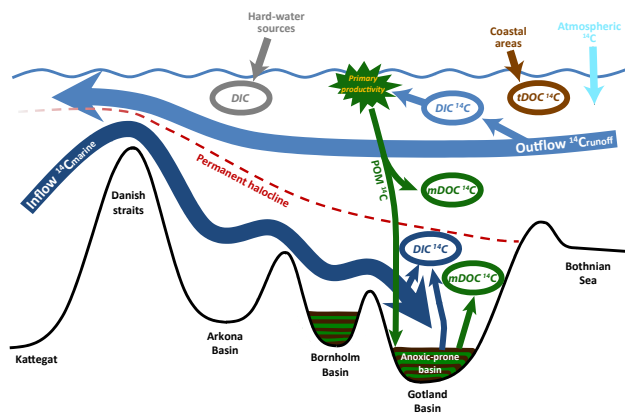
Fig. 2. Graphical representation of various ^{14}C source pathways within the Baltic Sea (see text for detailed explanation). Abbreviations are as follows: tDOC = terrestrial dissolved organic carbon, DIC = dissolved inorganic carbon, mDOC = marine dissolved organic carbon, and POM = particulate organic matter.

Rößler et al. (2011) carried out ^{14}C analysis on foraminifera tests and bulk sediment deposited at the same stratigraphic levels in Baltic Sea cores, and found that the bulk sediment age varied greatly when compared to the foraminifera age, being anywhere between 455 ^{14}C yr and 1090 ^{14}C yr older. This difference is typical for a coastal location, where continual changes in sediment source are common. It is recommended that bulk sediment ^{14}C dating in the Baltic Sea is avoided whenever possible. While the shells of calcifying organisms such as molluscs and foraminifera are generally a better source of material for ^{14}C dating, one still has to take the possibility of a species specific $R(t)$ into account (e.g. Ascough et al., 2005b; Philipssen and Heinemeier, 2013) and the possibility of metabolic carbon contributing to shell biomineralisation (Tanaka et al., 1986). Using advanced ^{14}C measurement techniques (e.g. Ruff et al, 2010; Wacker et al., 2013), it may in the future be possible to ^{14}C date very small samples containing phytoplankton, the ^{14}C content of which can reflect ambient seawater DIC (Tanaka et al., 1986).

2.3 Previous Baltic Sea reservoir age estimates

Modern anthropogenic ^{14}C production due to 20th century nuclear bomb testing has made it difficult to determine the natural, pre-bomb $R(t)$ of modern samples, so only a limited number of studies on the spatial distribution of reservoir ages in the Baltic Sea area have been carried out. Most studies have been based on ^{14}C dating of pre-bomb specimens of known calendar age. ^{14}C dating of four pre-bomb seaweed samples sourced from just off the southeast Swedish coast yielded a mean $R(t)$ of 255 ± 35 ^{14}C yr (Berglund, 1964; Engstrand, 1965), recalculated in this study using IntCal09. ^{14}C dates on seal bones in the north of the Baltic Sea yielded $R(t)$ values of approximately 300 ^{14}C yr (Olsson, 1980). These $R(t)$ estimates are all in relatively shallower

water and therefore from the outflowing water mass of the Baltic Sea. In the case of seal bones, it is difficult to constrain the exact environment that $R(t)$ reflects, because seals can move from area to area and have a varied diet. Such material most likely reflects a mix of $R(t)$ from multiple sources/areas. Lougheed et al. (2012) compared ^{14}C determinations on benthic foraminifera to an independent age model based on palaeomagnetic secular variation (PSV) at a deep location in the Gotland Basin (Fig. 1a) and found that reservoir ages decreased throughout the Holocene, possibly due to isostatically induced shallowing of the Baltic Sea basin and a concomitant reduction in ^{14}C$_{marine}$ influence. Just outside the Baltic Sea, Heier-Nielsen et al. (1995) analysed pre-bomb mollusc shells of known calendar age in marine waters in the Skagerrak and Kattegat (Fig. 1a). $R(t)$ values there were found to vary moderately, from 245 ± 56 to 527 ± 60 ^{14}C yr. The salinity of the investigated locations was not reported. $R(t)$ values reported for Danish fjords in limestone areas were found to be significantly higher, with values between 363 ± 67 and 901 ± 58 ^{14}C yr. The authors attributed this difference to the influence of a hard-water effect from groundwater sources in the Danish fjord environments, where calcareous bedrock is prevalent. Olsen et al. (2009) also found a significant hard-water effect in other Danish fjords with similar bedrock.

$R(t)$ uncertainties in the Baltic Sea are a recognised problem and the problems associated with bulk sediment ^{14}C dates have been known for quite some time (e.g. Olsson, 1979). However, Baltic Sea researchers have nonetheless continued to carry out ^{14}C dating on bulk sediment as there is often no other choice. Commonly, an $R(t)$ correction using some form of regional estimate is applied to bulk dates, usually between 300 and 400 ^{14}C yr (e.g. Kotilainen et al., 2000; Emeis et al., 2003). Such $R(t)$ estimates are derived from studies involving marine macrofossils and it is questionable whether these estimates can be applied to bulk sediment, as the ^{14}C source pathways for bulk sediment and marine macrofossils differ. In other recent Baltic Sea studies, the understandable decision is made not to employ any $R(t)$ correction to bulk dates at all, due to a lack of information thereon (e.g. Sohlenius et al., 1996; Zillén et al., 2008; Willumsen et al., 2013; Reinholdsson et al., 2013) However, it is known that bulk dates do yield older ages, so some correction should be applied. In many Baltic Sea studies, and also in many other marine studies worldwide, no 1 σ error uncertainty is included for $R(t)$, resulting in age models with unrealistically optimistic confidence intervals.

3 Methods

3.1 Collection of materials

Mollusc shells were retrieved from the collections of the Swedish Museum of Natural History (*Naturhistoriska*

riksmuseet) in Stockholm and the Finnish Museum of Natural History (*Luonnontieteellinen keskusmuseo*) at the University of Helsinki. Selection criteria were based on age, sample location and species type. Museum lot numbers can be found in the Supplement.

To ensure a representative salinity transect covering multiple sub-basins, shells were selected from multiple Baltic Sea sub-basins, from both above and below the Baltic Sea permanent halocline (Fig. 1b), from both mid-basin and near-coast areas. Only mollusc shells with a known collection date prior to 1950 AD were selected (Table 1), ensuring the selection of pre-bomb molluscs. Approximately 1/3 of the samples are from the period 1890–1950 AD, meaning that the Suess effect (dilution of atmospheric ^{14}C due to fossil fuel burning) may affect these samples (Ascough et al., 2005a). The mollusc shells selected were originally collected for zoological studies, meaning that the original investigators were interested in live specimens. Shells with evidence of having been alive at the time of collection were chosen, i.e. some organic material was still remaining and the lustre of the shell indicated that the shell was alive at the time of collection. In this way, one can be somewhat confident that the date of collection is close to the date of death of the mollusc and the outermost (youngest) material of the shell was subsampled for analysis. Care was taken to select mollusc shells whereby the collection location was well constrained (i.e. the ship logs contained reliable navigational data). Depths reported are from the museum database sourced from the ship logs and were checked against modern bathymetry data.

The euryhaline mollusc *Macoma balthica* was selected when possible. This species is abundant in the Baltic Sea and it was preferably selected to ensure species consistency within the study. *Macoma balthica* has a typical lifespan of 5–10 yr and can live at water depths as deep as 190 m (Budd and Rayment, 2001). In locations where *Macoma balthica* was not available, the molluscs *Arctica islandica*, *Astarte borealis*, *Astarte elliptica*, *Astarte montagui*, *Macoma calcarea* and *Mya arenaria* were selected. Additionally, the freshwater snail *Theodoxus fluviatilis* was selected at an inlet location (location 18, see Fig. 1).

3.2 Radiocarbon dating and calculation of reservoir ages

Between 10 % and 30 % of the surface of the subsampled shell material was etched away in 0.1 M HCl at 80 °C for about 5 h, resulting in approximately 15–20 mg of material per sample. Samples were subsequently graphitised. CO_2 was released from the pre-treated material through acidification with 85 % H_3PO_4. This CO_2 was then reduced to elementary C with H gas over a hot Fe surface (ca. 600 °C). Graphitised samples were subsequently measured for ^{14}C at the Lund University Radiocarbon Dating Laboratory single stage accelerator mass spectrometry (SSAMS) facility.

$R(t)$ values are calculated using the IntCal09 calibration curve (Reimer et al., 2009). The radiocarbon determination for each shell (^{14}C$_{shell}$) is assigned a calendar age (t) based on the sample collection date. The corresponding expected IntCal09 ^{14}C age (^{14}C$_{IntCal09}$) for the shell's calendar age (t) is then determined using the IntCal09 calibration curve. $R(t)$ (Table 1) is calculated as the offset from the IntCal09 calibration curve, as follows:

$$R(t) = {}^{14}C_{shell}(t) - {}^{14}C_{IntCal09}(t).$$

Reservoir age is discussed in this study as $R(t)$, using the offset from the atmospheric IntCal09 curve, due to many of the samples coming from very low salinity areas with little marine influence. However, for comparison with other studies, reservoir ages are also reported in the supplementary data as ΔR, the offset from the Marine09 calibration curve (Reimer et al., 2009), calculated using the same methodology, whereby ^{14}C$_{Marine09}(t)$ replaces ^{14}C$_{IntCal09}(t)$ to produce ΔR:

$$\Delta R = {}^{14}C_{shell}(t) - {}^{14}C_{Marine09}(t),$$

where 1σ errors for $R(t)$ and ΔR are calculated as a propagation of the 1σ errors associated with ^{14}C$_{shell}(t)$ and ^{14}C$_{IntCal09}(t)$ or ^{14}C$_{Marine09}(t)$.

3.3 Stable isotope analysis

Some of the shell material that was pretreated for ^{14}C analysis was set aside and measured for stable oxygen and carbon isotopes at the Faculty of Earth and Life Sciences (FALW) at Vrije Universiteit (VU), Amsterdam. Samples were analysed using a Thermo Finnigan Delta+ mass spectrometer equipped with a GASBENCH II preparation device, using approximately 20–50 µg of $CaCO_3$ sample. Isotope values are reported as δ^{13}C and δ^{18}O, relative to the Vienna–Peedee Belemnite (V-PDB) standard. The reproducibility of routinely analysed lab $CaCO_3$ standards is better than 0.1 ‰ (1σ) for both δ^{18}O and δ^{13}C.

3.4 Bottom salinity estimates

Bottom salinity in the Baltic Sea is strongly controlled by both water depth and proximity to the marine inflow water source; locations closer to the marine inflow source at the Danish sills tend to have higher salinity, and locations below the halocline have higher salinity than those above. Bottom salinity estimates were ascertained from a Baltic Sea model by Jacob Carstensen (HELCOM, 2013) based on observational data, which takes the in?uence of bathymetry upon bottom water salinity into account. While many of the samples selected are from the late 19th century, observational data from this period was not sufficient to develop bottom salinity maps. The mean bottom salinity for the annual data from the period 1900–1940 AD is therefore used and a one by one

Table 1. Selected data for all locations. Additional data can be found in the Supplement.

Loc. #	Species	Coordinates °N, °E	Depth[a] m	Average salinity[b] ‰±1σ	Nov. temp[c] °C	Yr of death, t yr AD	^{14}C IntCal09(t) ^{14}C yr BP ±1σ	Lund AMS Lab code	Shell ^{14}C age ^{14}C yr BP ±1σ	$R(t)$ ^{14}C yr ±1σ	δ^{13}C$_{aragonite}$ ‰ V-PDB ±1σ	δ^{18}O$_{aragonite}$ ‰ V-PDB ±1σ
1	*Arctica islandica*	54°47′, 10°25′	24	21.80±1.20	10.23	1932	129±7	LuS-9965	305±50	176±50	−0.16±0.1	0.11±0.1
2	*Astarte montagui*	54°31′, 11°49′	19	17.12±1.00	9.10	1888	98±7	LuS-9964	400±50	302±50	1.93±0.1	−0.49±0.1
3	*Arctica islandica*	54°46′, 12°22′	17	10.72±2.35	8.97	1878	104±8	LuS-9970	420±50	316±51	0.01±0.1	−1.00±0.1
4	*Macoma balthica*	55°19′, 12°47′	11	8.52±0.36	9.12	1878	104±8	LuS-10179	730±50	626±51	0.78±0.1	−4.18±0.1
5	*Macoma balthica*	55°00′, 13°24′	46	18.79±3.12	10.71	1878	104±8	LuS-9957	480±50	376±51	−0.03±0.1	−2.02±0.1
6	*Macoma balthica*	55°10′, 13°49′	47	14.79±3.56	10.41	1878	104±8	LuS-9976	410±45	306±46	0.06±0.1	−1.80±0.1
7	*Astarte borealis*	55°11′, 14°13′	49	13.14±3.14	9.89	1878	104±8	LuS-9967	320±50	216±51	2.30±0.1	−2.74±0.1
8	*Macoma balthica*	55°05′, 14°34′	22	8.31±1.16	9.16	1878	104±8	LuS-9975	430±45	326±46	−0.20±0.1	−2.64±0.1
9	*Astarte elliptica*	55°16′, 14°33′	49	11.81±1.41	9.27	1882	104±8	LuS-9966	365±50	261±51	1.68±0.1	−1.22±0.1
10	*Astarte borealis*	55°18′, 15°02′	71	15.18±0.97	7.26	1882	104±8	LuS-9962	270±45	166±46	1.40±0.1	−1.15±0.1
11	*Macoma calcarea*	55°17′, 15°47′	101	15.13±1.05	6.52	1878	104±8	LuS-9969	490±50	386±51	−1.85±0.1	−0.58±0.1
12	*Macoma balthica*	55°47′, 16°02′	54	12.60±0.97	6.46	1878	104±8	LuS-9956	370±50	266±51	0.15±0.1	−2.04±0.1
13	*Macoma balthica*	56°05′, 15°51′	9	7.19±0.23	7.29	1882	104±8	LuS-10182	270±50	166±51	0.08±0.1	−3.89±0.1
14	*Macoma balthica*	55°24′, 16°58′	45	8.31±0.71	6.94	1878	104±8	LuS-9972	390±60	286±61	−1.09±0.1	−1.14±0.1
15	*Macoma balthica*	55°50′, 16°54′	41	7.26±0.22	6.67	1878	104±8	LuS-10180	480±45	376±46	0.16±0.1	−3.30±0.1
16	*Astarte borealis*	55°10′, 17°43′	67	7.40±0.33	5.24	1878	104±8	LuS-9953	295±50	191±51	1.07±0.1	−2.28±0.1
17	*Mya arenaria*	54°41′, 18°45′	12	7.29±0.16	8.86	1931	129±7	LuS-10183	485±50	356±50	0.37±0.1	−6.18±0.1
18	*Theodoxus fluviatilis*	57°45′, 16°39′	2	6.78±0.16	6.12	1846	114±8	LuS-9968	1570±50	1456±51	−3.34±0.1	−6.23±0.1
19	*Macoma balthica*	57°32′, 17°16′	133	9.40±0.49	4.65	1879	104±8	LuS-9974	340±50	236±51	−2.31±0.1	−2.51±0.1
20	*Macoma balthica*	57°38′, 18°15′	36	6.93±0.17	6.02	1881	104±8	LuS-9955	1200±50	1096±51	−0.07±0.1	−4.10±0.1
21	*Macoma balthica*	57°36′, 18°50′	33	6.98±0.16	6.24	1881	104±8	LuS-10181	970±50	866±51	−0.28±0.1	−3.55±0.1
22	*Astarte borealis*	57°21′, 19°43′	187	10.56±0.50	5.18	1879	104±8	LuS-9963	485±50	381±51	0.71±0.1	−1.94±0.1
23	*Macoma balthica*	57°14′, 20°14′	182	10.69±0.48	5.24	1879	104±8	LuS-9959	970±50	866±51	0.16±0.1	−4.49±0.1
24	*Macoma balthica*	56°30′, 20°58′	8	7.03±0.16	8.78	1928	129±7	LuS-9958	870±50	741±50	−2.77±0.1	−5.73±0.1
25	*Macoma balthica*	57°52′, 24°21′	1	5.33±0.40	6.28	1926	132±7	LuS-9971	705±50	573±50	−3.24±0.1	−6.41±0.1
26	*Macoma balthica*	59°40′, 18°55′	1	6.03±0.16	5.96	1906	84±7	LuS-9973	270±50	186±50	1.57±0.1	−6.26±0.1
27	*Macoma balthica*	60°06′, 19°57′	1	6.02±0.09	5.87	1939	172±8	LuS-9952	360±45	188±46	−1.15±0.1	−4.34±0.1
28	*Macoma balthica*	60°07′, 24°46′	19	5.72±0.15	5.81	1893	78±7	LuS-9961	250±50	172±50	0.28±0.1	−4.28±0.1
29	*Macoma balthica*	63°25′, 20°47′	40	4.42±0.09	4.71	1934	154±8	LuS-9960	265±50	111±51	2.08±0.1	−6.13±0.1
30	*Macoma balthica*	63°04′, 20°50′	2	4.79±0.09	4.72	1934	154±8	LuS-9954	270±45	116±46	−0.33±0.1	−6.07±0.1

[a] Depth as reported in museum records when available. Locations 17, 18, 24, 25, 26 and 27 are estimated depths using IOC et al. (2003) bathymetry. [b] Average 1900–1940 water salinity from Carstensen et al. (2013) dataset, except for locations 1, 2, 25 and 28 which are from the Janssen et al. (1999) 1900–1996 dataset, see Fig. 1b. [c] Average November water temperature for 1900–1996 from Janssen et al. (1999) dataset. Annual temperature data and data for other months (and δ^{18}O$_{wtr}$) can be found in the Supplement.

minute latitude and longitude bottom salinity map was produced (Fig. 1b), along with the standard deviation of the annual data, allowing mean bottom salinity values and associated 1σ errors to be assigned to the sample locations. The salinity observations were carried out at irregular intervals over the period 1900–1940 AD, so not all basins are represented by all years in the dataset. The number of years (n) used to compute the 1900–1940 AD mean and standard deviation for each basin is as follows; Arkona Basin ($n = 12$), Bornholm Basin ($n = 32$), Gotland Basin ($n = 36$), Gulf of Finland ($n = 36$), Bothnian Sea ($n = 36$) and Bothnian Bay ($n = 33$). Larger 1σ values are found in the Arkona Basin salinity data, due to the proximity of this basin to the source of sporadic inflows of marine water from the Danish straits.

Sample locations 1, 2, 25 and 28 are not covered by the HELCOM (2013) dataset. The estimations for these locations are taken from the annual mean of a mean monthly 1900–1996 AD dataset by Janssen et al. (1999). This dataset has a spatial resolution of 10 min latitude by 6 min longitude, with 18 vertical levels. Errors (1σ) are based on the standard deviation of the mean monthly 1900–1996 (January–December) data. All temperature data in this study is also taken from the Janssen et al. (1999) dataset.

4 Results

4.1 All samples (locations 1–30)

In the following results, all samples (from locations 1–30) are collectively discussed.

4.1.1 $R(t)$ vs. average salinity (all samples)

$R(t)$ is found to fluctuate between 111 ± 51 and 1456 ± 51 ^{14}C yr (Table 1). No statistically significant correlation can be found between all $R(t)$ results and average salinity (Figs. 3a and 4a), although two groups can be visually identified; samples where $R(t) > 500$ ^{14}C yr and samples where $R(t) < 500$ ^{14}C yr. Of the seven samples whereby $R(t) > 500$ ^{14}C yr (locations 4, 18, 20, 21, 23, 24 and 25), six are from locations that are within 10 km of the coast (locations 4, 18, 20, 21, 24 and 25). It is further noted that the two samples with lowest $R(t)$ values (locations 29 and 30) are the two northernmost samples and are associated with the two lowest average salinity values (Fig. 3a, Table 1).

4.1.2 $R(t)$ vs. $\delta^{13}C_{aragonite}$ (all samples)

A weak, but significant, correlation is found between $R(t)$ and $\delta^{13}C_{aragonite}$ (Figs. 3b and 4a), whereby $R = -0.48$ and $p = 4 \times 10^{-3}$. The three samples with the most depleted $\delta^{13}C_{aragonite}$ values (locations 18, 24 and 25) are all samples with $R(t) > 500$ ^{14}C yr, but other samples with similarly high $R(t)$ (locations 4, 20, 21 and 23) do not display atypical $\delta^{13}C_{aragonite}$ values (Fig. 3b). No statistically significant
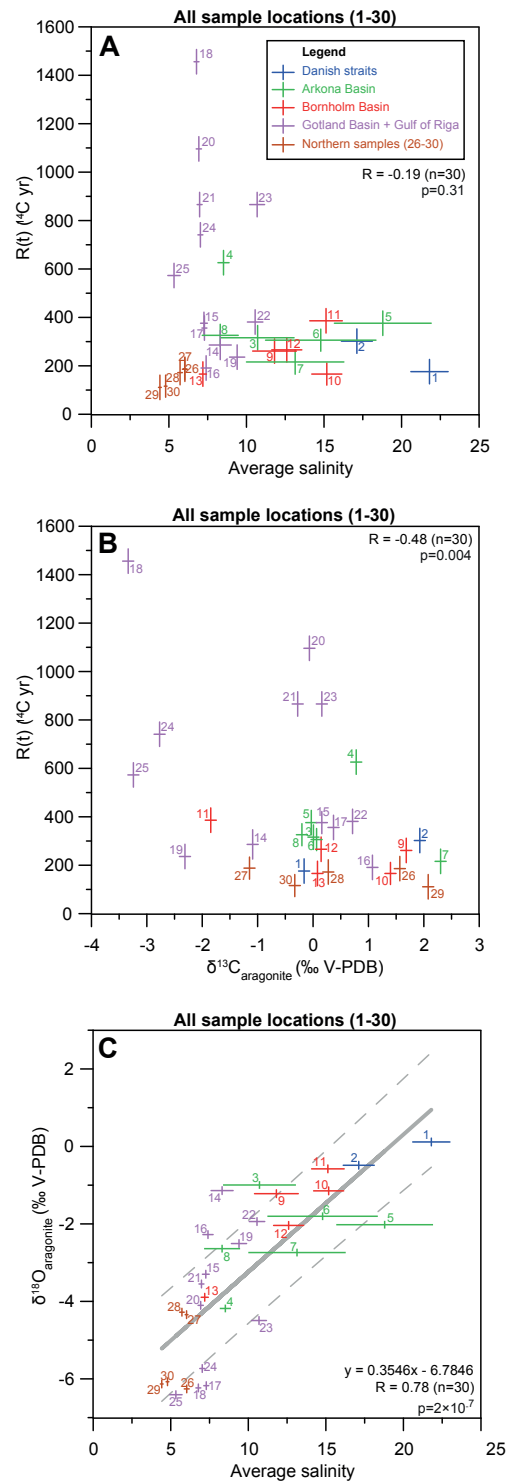

Fig. 3. (A) $R(t)$ vs. average salinity for all samples. 1σ error bars. **(B)** $R(t)$ vs. $\delta^{13}C_{aragonite}$ for all samples. 1σ error bars. **(C)** $\delta^{18}O_{aragonite}$ vs. average salinity for all samples. 1σ error bars. Linear regression (grey line) with 1σ confidence intervals (dashed line) also shown. For all figures: numbers next to data points indicate sample location numbers following Fig. 1 and Table 1.
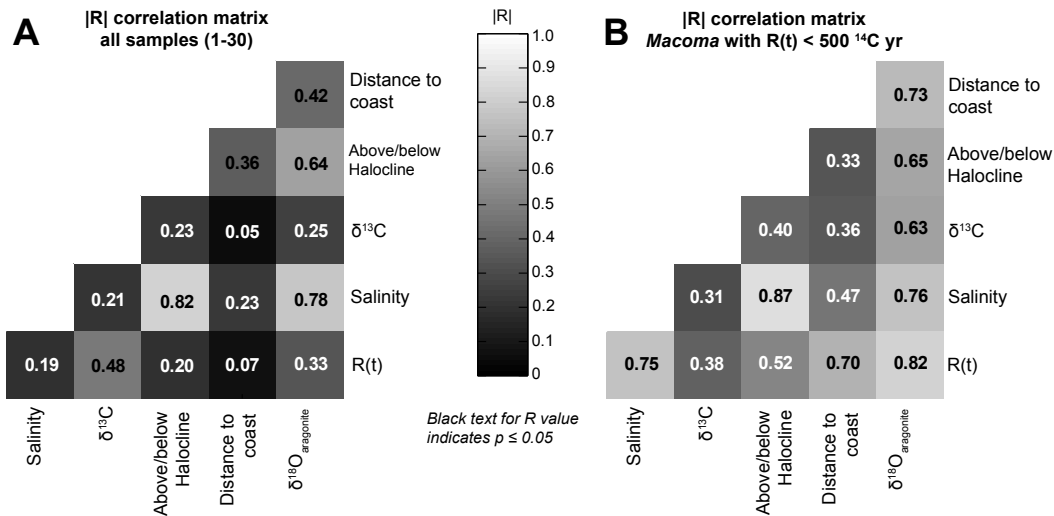
Fig. 4. (A) Correlation coefficient matrix for all sample locations. **(B)** Correlation coefficient for all *Macoma* samples with $R(t) < 500$ ^{14}C yr. For both figures: values shown are absolute values of correlation coefficient R, when written with black text $p \leq 0.05$. Correlations based on values in Table 1 and in Supplement.

correlation is found between $\delta^{13}C_{aragonite}$ and average salinity (Fig. 4a).

4.1.3 $\delta^{18}O_{aragonite}$ vs. average salinity (all samples)

A statistically significant correlation coefficient ($R = 0.78$, $p = 2 \times 10^{-7}$) is found between $\delta^{18}O_{aragonite}$ and average salinity for all samples (Figs. 3c and 4a). This correlation suggests that $\delta^{18}O_{aragonite}$ can be approximately described using a basic linear mixing model between $\delta^{18}O_{marine}$ and $\delta^{18}O_{runoff}$, even when one does not correct $\delta^{18}O_{aragonite}$ for temperature fractionation effects (Grossman and Ku, 1986).

4.2 *Macoma* samples with $R(t) < 500$ ^{14}C yr

Biogenic carbon can contribute to shell biomineralisation (Tanaka et al., 1986), while species type has been shown to influence $R(t)$ (Ascough et al., 2005b; Philipssen and Heinemeier, 2013), possibly due to the influence of carbon sources in diet and biomineralisation. In order to exclude such effects as much as possible, the following results include only samples from the *Macoma* genus (which comprises 2/3 of the samples used in this study), whereby all locations with $R(t) > 500$ ^{14}C yr (i.e. suspected hard-water locations, see discussion) have been excluded.

4.2.1 *Macoma* $R(t)$ vs. average salinity

The selection of *Macoma* samples with $R(t) < 500$ ^{14}C yr results in a linear relationship with a statistically significant correlation ($R = 0.75$, $p = 1 \times 10^{-4}$) between $R(t)$ and average salinity (Figs. 4b and 5a), suggesting that a basic linear mixing model between $^{14}C_{runoff}$ and $^{14}C_{marine}$ provides a valid estimation for *Macoma* $R(t)$ in locations not influenced by hard water.

4.2.2 *Macoma* $R(t)$ vs. average salinity (Northern samples only)

A very robust linear correlation ($R = 0.99$, $p = 5 \times 10^{-4}$) between $R(t)$ and average salinity is found for all northern region samples (Fig. 5b), all of which are of the species *Macoma balthica*.

4.2.3 Late 19th and early 20th century *Macoma* shell aragonite inferred $R(t)$ map

Using the bottom salinity map (Fig. 1b) and the regression equations in Fig. 5a and b, a map of inferred Baltic Sea $R(t)$ values for late 19th and early 20th century *Macoma* shell aragonite with $R(t) < 500$ ^{14}C yr can be produced (Fig. 6), whereby the regression equation in Fig. 5b is used for the northern basins (north of the black dotted line in Fig. 6) and the regression equation in Fig. 5a is used for all other basins. The 1σ confidence interval shown on Fig. 5a suggests that, generally, a 1σ error of approximately ± 75 ^{14}C yr should be used for $R(t)$ estimates shown on the map in Fig. 6, although one may consider using a smaller 1σ error estimate in northern areas. One should take into account that the $R(t)$ values shown in the map were calculated using average observed salinity – in deeper areas subject to periodic marine inflow events, such as the Arkona, Bornholm and Gotland deeps, one may encounter sporadic increases in salinity.

4.2.4 *Macoma* $R(t)$ vs. $\delta^{18}O_{aragonite}$

A statistically significant correlation ($R = 0.82$, $p = 2 \times 10^{-4}$) is also found between *Macoma* $R(t)$ and $\delta^{18}O_{aragonite}$ for all locations where $R(t) < 500$ ^{14}C yr (Fig. 5c). The existence of this correlation suggests that $\delta^{18}O_{aragonite}$ can be

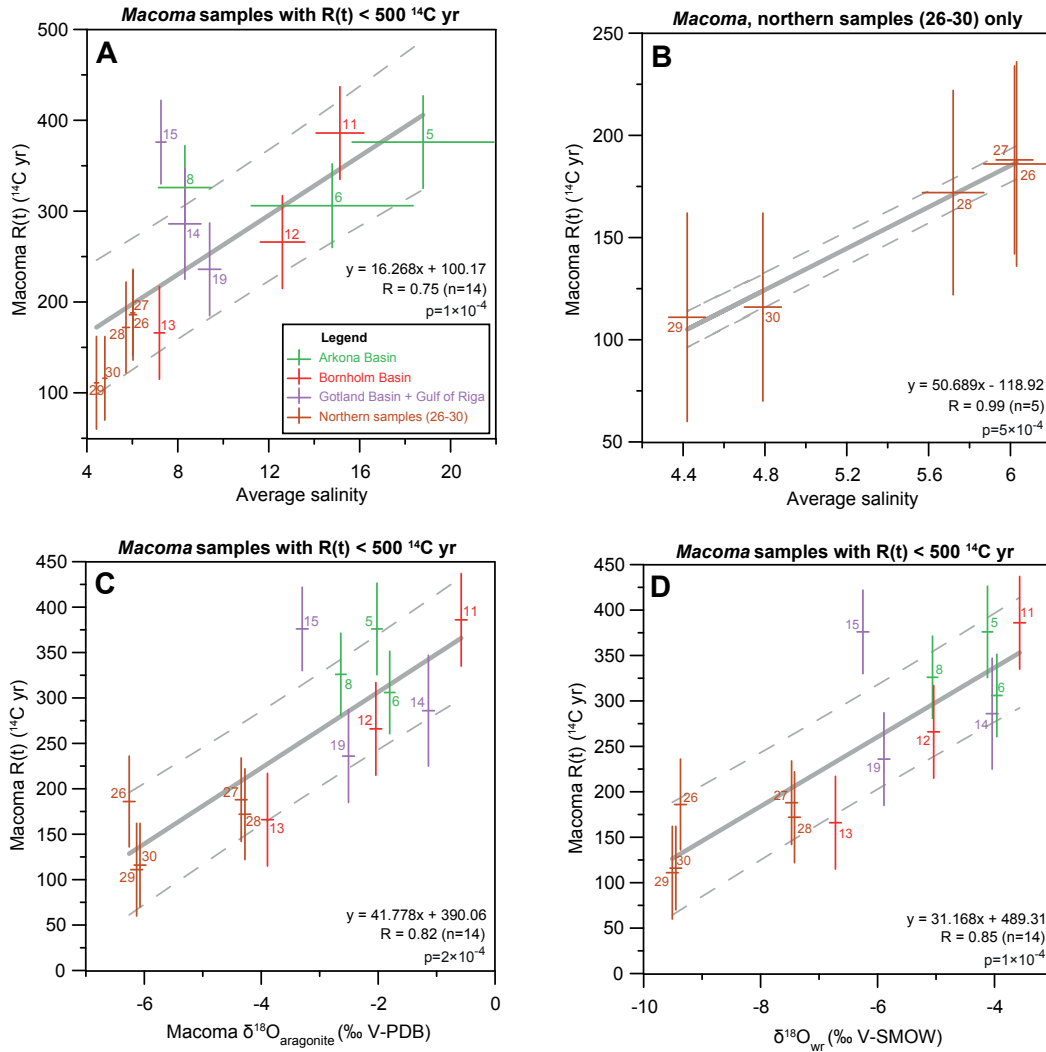**Fig. 5. (A)** $R(t)$ vs. average salinity for *Macoma* samples with $R(t) < 500\,^{14}$C yr. **(B)** $R(t)$ vs. average salinity for northern samples (locations 26–30) only. **(C)** $R(t)$ vs. $\delta^{18}O_{\text{aragonite}}$ for *Macoma* samples with $R(t) < 500\,^{14}$C yr. **(D)** $R(t)$ vs. $\delta^{18}O_{\text{wr}}$ (water reconstructed) for *Macoma* samples with $R(t) < 500\,^{14}$C yr, based on correction of $\delta^{18}O_{\text{aragonite}}$ for the temperature fractionation effect (see Sect. 4.2.5). For all figures: all error bars are $1\,\sigma$. Linear regression (grey line) with $1\,\sigma$ confidence intervals (dashed line) also shown in some cases. Numbers next to data points indicate sample location numbers following Fig. 1 and Table 1.

used to estimate $R(t)$, whereby the $1\,\sigma$ confidence interval in Fig. 5c suggests that a $1\,\sigma$ error of approximately $\pm 65\,^{14}$C yr should be used for these $R(t)$ estimates. The existence of such a correlation is to be expected, seeing as *Macoma* $R(t)$ vs. average salinity and a $\delta^{18}O_{\text{aragonite}}$ vs. average salinity relationships were previously found.

4.2.5 *Macoma R(t)* vs. $\delta^{18}O_{\text{wr}}$

One can correct $\delta^{18}O_{\text{aragonite}}$ for temperature fractionation effects in mollusc aragonite using Eq. (3) in Grossman and Ku (1986), which allows for $\delta^{18}O_{\text{wr}}$ (water reconstructed) to be inferred, with 0.27 ‰ subsequently being added for conversion to the Vienna Standard Mean Ocean

Water (V-SMOW) scale (Hut, 1987). $\delta^{18}O_{\text{wr}}$ can be expected to be a better salinity proxy, seeing as the aforementioned temperature fractionation effects are removed. When this correction is done using average 1900–1996 November water temperature (Table 1), a statistically significant correlation is found between *Macoma* $R(t)$ and $\delta^{18}O_{\text{wr}}$ (Fig. 5d), whereby $R = 0.85$ and $p = 1 \times 10^{-4}$, an improvement over the correlation coefficient previously found for Macoma $R(t)$ vs. $\delta^{18}O_{\text{aragonite}}$ ($R = 0.82$, $p = 2 \times 10^{-4}$). Fractionation corrections using average annual, summer or winter temperature result in lower correlation coefficients, suggesting that the *Macoma* material used for ^{14}C dating (which contained multiple growth rings) is most sensitive to fractionation correction using autumn (November) water temperatures. When one is
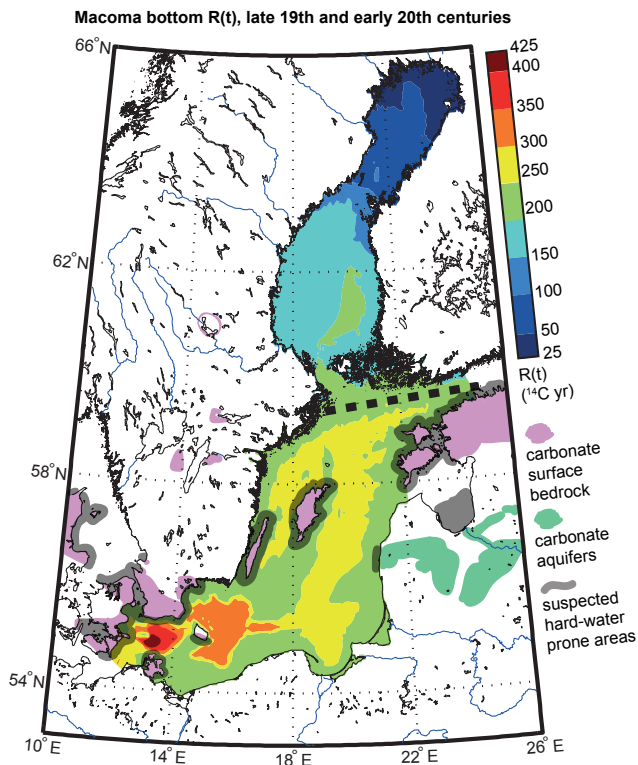
Fig. 6. Map of $R(t)$ for all Macoma samples with $R(t) < 500$ [14]C yr, calculated using salinity map in Fig. 1b and regression equations in Fig. 5a and b. Areas south of dashed black line calculated using regression equation in Fig. 5a, areas north of dashed black line calculated using regression equation in Fig. 5b. Estimated 1σ error is ± 75 ^{14}C yr. Also shown are carbonate bedrock and aquifers (pink and light green areas, respectively, following Stephens et al., 1994; Kalberg et al., 2007; BGR Hannover et al., 2008).

able to correct for temperature fractionation in $\delta^{18}O_{\text{aragonite}}$ in this way, the resulting $\delta^{18}O_{\text{wr}}$ should preferentially be used to estimate *Macoma* $R(t)$, using the linear regression equation in Fig. 5d. The 1σ confidence interval in Fig. 5d suggests that a 1σ error of approximately ± 60 ^{14}C yr should be used for these $R(t)$ estimates.

5 Discussion

5.1 Baltic Sea $R(t)$ and hard-water effects

Of the 30 sample locations analysed in this study, seven (locations 4, 18, 20, 21, 23, 24 and 25) resulted in an unusually large $R(t)$, greater than 500 ^{14}C yr. The largest $R(t)$ was at location 18, a coastal inlet location and the only location where no bivalve mollusc was available for analysis. The species analysed was *Theodoxus fluviatilis*, a freshwater snail that lives on stony substrata, such as pebbles and rocks, and can therefore incorporate ^{14}C depleted carbonates from rock material into its diet, resulting in a significant hard-water

effect. Of the six other locations with $R(t) > 500$ [14]C yr (locations 4, 20, 21, 23, 24 and 25), all but location 23 were from coastal areas (< 10 km from coast). All of these high $R(t)$ coastal locations are located on or near coasts dominated by limestone bedrock or aquifers (Fig. 1b), which can contribute DIC of infinite ^{14}C age to the local groundwater (Paukstys and Narbutas, 1996). Of particular note is the River Daugava, which flows through areas dominated by hard-water aquifers on its way to the Gulf of Riga (Fig. 1b). Location 23, from the Gotland Deep, is the only non-coastal sample with $R(t) > 500$ [14]C yr. One possible explanation for this is that location 23 is situated deep under the halocline in the Gotland basin, a location that is often anoxic and where laminae of (organic) carbon can be preserved. Such basins can become periodically oxic, creating conditions in which molluscs can thrive. In such conditions, previously accumulated (organic) carbon can dissolve and therefore contribute older ^{14}C to the dissolved carbon pool in sediment pore waters, which is then biomineralised by molluscs.

The presence of hard water at locations near to the coast should be taken into account when ^{14}C dating shell material. For these reasons, coastal locations are likely to be influenced by hard water from land areas with carbonate outcrops or karst features are indicated with dark shading in the *Macoma* $R(t)$ map in Fig. 6. It is stressed that this indication is only a guide. More research is needed to determine exactly how far out to sea the influence of the hard water-effect can extend, seeing as this can depend on local runoff patterns and groundwater discharge. It is noted that the correlation between *Macoma* $R(t)$ and salinity is more robust in the northern basins (Fig. 5b) when compared to all basins (Fig. 5a). The northern basins are found to be almost free of carbonate bedrock, which is generally more prevalent in the southern parts of the Baltic (Fig. 1b). The generally less robust correlation between *Macoma* $R(t)$ and salinity for all basins when compared to the carbonate-poor northern basins suggests that there is some hard-water variability present in the southern basins, even in locations further from the coast. Additionally, basins that are periodically anoxic should also be treated as uncertain areas for estimating $R(t)$, as the influence of previously accumulated laminae of old carbon upon $R(t)$ is still not well understood.

5.2 Salinity as a *Macoma* $R(t)$ proxy

When one knows salinity – and in the absence of hard-water effects – the linear regression equation in Fig. 5a can be used to estimate *Macoma* $R(t)$ for the Baltic Sea in general, with a 1σ error of approximately ± 75 ^{14}C yr. A basic linear mixing model between [14]C_{marine} and [14]C_{runoff} end-members is assumed, and a simple extrapolation of the regression line shown in Fig. 5a suggests that water with a salinity of 30 PSU (i.e. almost full marine water, representative of the [14]C_{marine} end-member) should have an $R(t)$ value of approximately 590 ± 75 ^{14}C yr. This value is slightly higher than the $R(t)$

found in previous studies of mollusc shells from deeper Kattegat and Skagerrak waters, which have a full marine salinity of 30 PSU and greater, where $R(t)$ values of between 370 ± 64 and 527 ± 60 ^{14}C yr were reported (Heier-Nielsen et al., 1995). This discrepancy could be due to a slightly increased hard-water effect in Baltic Sea waters, as marine inflow water from the Skagerrak and Kattegat must travel through the shallow Danish straits, an area dominated by limestone bedrock and associated runoff (Fig. 1b). It is of particular note that the regression equation in Fig. 5a infers a *Macoma* $R(t)$ of 220 ± 75 ^{14}C yr for the salinity values for the southeast Swedish coast at Blekinge, and this agrees well with the mean $R(t)$ value of 255 ± 35 ^{14}C yr previously found for four pre-bomb seaweed samples in that area (Berglund, 1964; Engstrand, 1965).

In the case of the northern basins (north of the black dotted line in Fig. 6), which are dominated by freshwater-sourced ^{14}C$_{runoff}$, the linear regression equation in Fig. 5b can be used for estimating *Macoma* $R(t)$, and a reduced 1σ error can be considered (Fig. 5b). This robust correlation suggests that *Macoma* $R(t)$ in the northern basins is governed by the interplay between runoff water well equilibrated with atmospheric ^{14}C and marine water influence, with minimal influence of hard-water effects. It is of note that the bedrock in the northern river catchment areas is free of limestone (Fig. 1b), meaning that one should not expect a significant hard-water contribution from these catchments. The gradient of the regression line for northern basins (Fig. 5b) is steeper than that for all basins (Fig. 5a), possibly due to different overall hard water conditions.

It should be noted that the regression equations in Fig. 5a and b are based on the *Macoma* genus of mollusc, which is abundant in the Baltic Sea. While these equations may be applicable when estimating $R(t)$ for other organisms that biomineralise $CaCO_3$ (e.g. other molluscs and foraminifera), in such cases one should consider increasing experimental errors appropriately, due to possible species-specific reservoir ages (Ascough et al., 2005b; Philipssen and Heinemeier, 2013). It is not recommended to use these equations in tandem with ^{14}C dates derived from bulk sediment samples.

When considering applying $R(t)$ values back through time, one must consider the fact that most of the Baltic Sea has become shallower throughout the Holocene, with continuously decreasing ^{14}C$_{marine}$ influence over the course of the past 7000–8000 yr. Consequently, this freshening has likely resulted in a time dependent decrease in $R(t)$ throughout the Holocene, with early Holocene values closer to the Skagerrak and Kattegat values (Lougheed et al., 2012). This decreasing trend should be taken into account when using the regression equations in Fig. 5a and b to estimate *Macoma* $R(t)$ downcore and, ideally, some form of palaeosalinity proxy should be employed. Possible temporal changes in the ^{14}C$_{marine}$ end-member should also be considered; while ocean circulation throughout the mid- to late Holocene has remained relatively stable, isostatic adjustment of the carbonate rich

bedrock at the Danish straits may have affected the overall hard-water contribution to the ^{14}C$_{marine}$ end-member water entering the Baltic basins. It can be assumed that the ^{14}C$_{runoff}$ end-member has remained well equilibrated with atmospheric ^{14}C throughout the Holocene. Finally, the regression equations discussed here apply for time periods after 8 ka BP, i.e. the Littorina stage of the Baltic Sea and later (e.g. Björck, 1995).

5.3 $\delta^{18}O_{aragonite}$ and $\delta^{18}O_{wr}$ as *Macoma* $R(t)$ proxies

Using the linear regression equation in Fig. 5c, it is possible to estimate palaeo-$R(t)$ for *Macoma* aragonite using $\delta^{18}O_{aragonite}$, due to the $\delta^{18}O_{aragonite}$ signal in the Baltic Sea being dominated by salinity. When doing so, three major assumptions are made: firstly, as is the case when using salinity as an $R(t)$ proxy, one assumes that the ^{14}C$_{marine}$ end-member remains somewhat constant throughout the history of the current stage of the Baltic Sea. Secondly, the assumption is made that the isotopic enrichment of the respective $\delta^{18}O_{marine}$ and $\delta^{18}O_{runoff}$ end-members remains somewhat constant. Changes in Holocene evapotranspiration in catchment areas could have effected oxygen isotope fractionation and consequently $\delta^{18}O_{runoff}$. The third assumption is that the temperature fractionation effect upon *Macoma* $\delta^{18}O_{aragonite}$ is minimal and has remained so throughout the Holocene. Caution must be urged when making such an assumption, because salinity and temperature values can be expected to have been different in the past, thus influencing the $\delta^{18}O_{marine}$ and $\delta^{18}O_{runoff}$ end-members, although one can assume that a large salinity gradient was present throughout the Littorina sea stage.

When (palaeo)temperature data are available, it is much more preferable to correct $\delta^{18}O_{aragonite}$ for temperature fractionation effects and to thus calculate $\delta^{18}O_{wr}$, which more accurately reflects the mixing between $\delta^{18}O_{marine}$ and $\delta^{18}O_{runoff}$, leading to a more robust *Macoma* $R(t)$ proxy (Fig. 5c and d). Such a correction is more challenging in shallower areas of the Baltic Sea, where the combination of a stratified water column and high seasonality means that large, intra-annual variations in the thermocline are common, which can affect the recording of $\delta^{18}O_{aragonite}$ by molluscs (e.g. Austin et al., 2006). In this study it has been found that Baltic Sea autumn (November) water temperature is the most suitable for correcting for temperature fractionation. However, multiple growth rings of shells were analysed, as subsampling was carried out with the aim of having sufficient material for AMS ^{14}C analysis. Discriminate sampling of seasonal growth rings, combined with seasonal temperature data, would likely lead to a better temperature fractionation correction for $\delta^{18}O_{aragonite}$. Locations located under the Baltic Sea thermocline can be expected to be less sensitive to intra-annual temperature variations.

Methods for estimating palaeo-$R(t)$ in the Baltic Sea are generally lacking, and $\delta^{18}O_{aragonite}$ and, preferably, $\delta^{18}O_{wr}$

provide a good approximate estimation for palaeo-$R(t)$ for *Macoma* shells. Errors (1σ) of approximately ±65 ^{14}C yr and ±60 ^{14}C yr are indicated for the $\delta^{18}O_{aragonite}$ and $\delta^{18}O_{wr}$ based $R(t)$ estimation methods, respectively. Additionally, the regression equation in Fig. 5d, which allows $\delta^{18}O_{wr}$ to be used to estimate *Macoma* $R(t)$, may be useful for estimating $R(t)$ in studies where $\delta^{18}O_{wr}$ is derived from other sources, such as foraminifera. In such cases, one must consider species-specific reservoir effects upon $R(t)$.

5.4 Wider implications of this Baltic Sea case study

The results of this study, which show that river runoff can greatly modify marine $R(t)$ in coastal areas, are important for other coastal locations around the world, where accurate ^{14}C geochronologies are required. When one controls for hard-water and species effects, a similar end-member mixing model for $^{14}C_{runoff}$ and $^{14}C_{marine}$ can be investigated for other coastal locations, whereby salinity or $\delta^{18}O$ can be used as proxies for $R(t)$.

The results also have consequences for previous reservoir age studies that have been carried out in coastal areas near large freshwater sources. For example, Bondevik et al. (2006) investigated shallow Norwegian coastal locations and used mollusc shells to reconstruct reservoir age during the last deglaciation, and assumed that these reservoir ages reflect North Atlantic water. The proximity of their study location to the large, oscillating Fennoscandian ice-sheet and associated freshwater fluxes makes such an assumption difficult because these fluxes can contribute to large changes in local reservoir age. Indeed, temporal changes of up to 3.5‰ in $\delta^{18}O_{aragonite}$ (not corrected for temperature fractionation) are found for molluscs at their coastal study site, changes which are not found in deep water sites (Bondevik et al., 1999), indicating a possible local variation in hydrographic conditions at the coastal site. A 3.5‰ change in $\delta^{18}O_{aragonite}$ for Baltic Sea molluscs (also not corrected for temperature fractionation) has been shown, in this study, to be equivalent to a salinity change of approximately 10 PSU (Fig. 3c) and an $R(t)$ change of approximately 150 ^{14}C yr (Fig. 5c). It is possible that the North Atlantic reservoir age variations described by Bondevik et al. (2006) are being significantly amplified by freshwater fluxes due to oscillations of the nearby Fennoscandian ice-sheet. It may, therefore, be better to estimate deglacial changes in North Atlantic reservoir age from study sites situated further from the coast and in deeper water (e.g. Austin et al., 2011).

One must also consider the consequences of this Baltic Sea study for reservoir age determinations that have been carried out on macrofossils from larger animals (e.g. whales and seals) that regularly move between waters of differing salinity, such as in studies by Gordon and Harkness (1992) and Mangerud et al. (2006). These determinations most likely reflect an average reservoir age for a large region where significant internal spatial variations may exist, especially in coastal areas.

6 Conclusions

Reservoir age analyses of pre-bomb mollusc shells across a strategic salinity transect in the Baltic Sea have been carried out. A number of these samples, in hard-water prone areas, produced much higher $R(t)$ values, most likely due to the influence of ^{14}C depleted carbon from carbonate bedrock.

A hydrographic control upon $R(t)$ can be found when one controls for sample genus and hard-water effect. Specifically, a statistically significant correlation is found between $R(t)$ and water salinity for all *Macoma* mollusc samples with $R(t) < 500$ ^{14}C yr, allowing water salinity to be used to infer *Macoma* $R(t)$ in locations not influenced by hard water (Fig. 6). Additionally, as $\delta^{18}O_{aragonite}$ is also indicative of hydrographic conditions, a similar correlation is also found between $\delta^{18}O_{aragonite}$ and $R(t)$, suggesting that $\delta^{18}O_{aragonite}$ can be used as an estimator for palaeo-$R(t)$ in the Baltic Sea. An increased correlation with $R(t)$ can be expected when $\delta^{18}O_{aragonite}$ is corrected for temperature fractionation effects; the resulting $\delta^{18}O_{wr}$ more accurately reflects the mixing between $\delta^{18}O_{marine}$ and $\delta^{18}O_{runoff}$. It is stressed that the correlations are based on 19th and 20th century pre-bomb *Macoma* shell aragonite in areas that are not prone to hard water influence. It is not recommended to use these mollusc-derived $R(t)$ estimates in tandem with bulk sediment samples.

The results of this Baltic Sea study are of great importance for researchers in the world's other coastal and estuarine locations, where moderation of marine $R(t)$ by freshwater runoff is also likely to be affected by spatial and temporal changes in hydrographic conditions and local carbon inputs. In such environments, researchers must take great care when estimating $R(t)$ and select a realistic 1σ error that sufficiently takes uncertainties into account.

Supplementary material related to this article is available online at: http://www.clim-past.net/9/1015/2013/cp-9-1015-2013-supplement.zip.

References

Adolphi, F.: Holocene temperature reconstruction in Baltic Sea sediments for the last 2000 years, using the biomarker TEX86, MSc Theis, 94 pp., Technical University Bergakademie, Freiburg, 2010.

Andersson, P. S., Wasserburg, G. J., and Ingri, J.: The sources and transport of Sr and Nd isotopes in the Baltic Sea, Earth Planet. Sc. Lett., 113, 459–472, 1992.

Ascough, P., Cook, G., and Dugmore, A.: Methodological approaches to determining the marine radiocarbon reservoir effect, Progr. Phys. Geogr., 29, 532–547, 2005a.

Ascough, P. L., Cook, G. T., Dugmore, A. J., Scott, E. M., and Freeman, S. P. H. T.: Influence of mollusc species on marine ΔR determinations, Radiocarbon, 47, 433–440, 2005b.

Austin, W. E. N., Cage, A. G., and Scourse, J. D.: Mid-latitude shelf seas: a NW European perspective on the seasonal dynamics of temperature, salinity and oxygen isotopes, Holocene, 16, 937–947, 2006.

Austin, W. E. N., Telford, R. J., Ninnemann, U. S., Brown, L., Wilson, L. J., Small, D. P., and Bryant, C. L.: North Atlantic reservoir ages linked to high Younger Dryas atmospheric radiocarbon concentrations, Global Planet. Change, 79, 226–233, 2011.

Berglund, B: The Post-Glacial Shore Displacement in Eastern Blekinge, Southeastern Sweden, in: Publications from the Institutes of Mineralogy, Paleontology and Quaternary Geology, University of Lund, Sweden, Sveriges Geologiska Undersökning (SGU), Stockholm, Ser C, Nr. 599, 1964.

BGR Hannover, EGS Brussels, UNESCO: International Hydrogeological Map of Europe (1 : 5,000,000), UNESCO Publishing, Paris, 2008.

Björck, S.: A review of the history of the Baltic Sea, 13.0–8.0 ka BP, Quaternary Int., 27, 19–40, 1995.

Bondevik, S., Birks, H. H., Gulliksen, S., and Mangerud, J.: Late Weichselian Marine 14C Reservoir Ages at the Western Coast of Norway, Quaternary Res., 52, 104–114, 1999.

Bondevik, S., Mangerud, J., Birks, H. H., Gulliksen, S., and Reimer, P.: Changes in North Atlantic Radiocarbon Reservoir Ages During the Allerød and Younger Dryas, Science, 312, 1514–1517, 2006.

Budd, G. and Rayment, W.: Macoma balthica. Baltic tellin, Marine Life Information Network: Biology and Sensitivity Key Information Sub-programme, available at: http://www.marlin.ac.uk/ (last access: 18 April 2013), Plymouth: Marine Biological Association of the United Kingdom, 2001.

Cage, A. G., Heinemeier, J., and Austin, W. E. N.: Marine radiocarbon reservoir ages in scottish coastal and fjordic waters, Radiocarbon, 48, 31–43, 2006.

Carstensen, J., Conley, D. J., Lophaven, S., Danielsson, Å., Rahm, L., and Toompuu, A.: Statistical Analysis and Modelling of Phytoplankton Dynamics: Exploitation of Data in the Nordic and Baltic Monitoring Programs, Nordic Council of Ministers, 2002.

Damon, P. E., Lerman, J. C., and Long, A.: Temporal fluctuations of atmospheric ^{14}C: causal factors and implications, Annual Rev. Earth Planet. Sc., 6, 457–494, 1978.

Ehhalt, D. H.: On the deuterium-salinity relationship in the Baltic Sea, Tellus, 21, 429–435, 1969.

Emeis, K.-C., Struck, U., Blanz, T., Kohly, A., and Voß, M.: Salinity changes in the central Baltic Sea (NW Europe) over the last 10 000 years, Holocene, 13, 411–421, 2003.

Engstrand, L. G.: Stockholm natural radiocarbon measurements VI, Radiocarbon, 7, 257–290, 1965.

Fröhlich, K., Grabczak, J., and Rozanski, K.: Deuterium and oxygen-18 in the baltic sea, Chem. Geol., 72, 77–83, 1988.

Gordon, J. E. and Harkness, D. D.: Magnitude and geographic variation of the radiocarbon content in Antarctic marine life: Implications for reservoir corrections in radiocarbon dating, Quaternary Sci. Rev., 11, 697–708, 1992.

Grossman, E. L. and Ku, T. L.: Oxygen and carbon isotope fractionation in biogenic aragonite: temperature effects, Chem. Geol., 59, 59–74, 1986.

Gustafsson, B. G. and Westman, P.: On the causes for salinity variations in the Baltic Sea during the last 8500 years, Paleoceanography, 17, 12.1–12.14, doi:10.1029/2000PA000572, 2002.

Heier-Nielsen, S., Heinemeier, J., Nielsen, H. L., and Rud, N.: Recent reservoir ages for Danish fjords and marine waters., Radiocarbon, 37, 875–882, 1995.

HELCOM: Approaches and methods for eutrophication target setting in the Baltic Sea region, Balt. Sea Environ. Proc., No. 133, 2013.

Hut, G.: Consultants' group meeting on stable isotope reference samples for geochemical and hydrological investigations, Report to the Director General, International Atomic Energy Agency, Vienna, April, 1987.

IOC, IHO, BODC: Centenary Edition of the GEBCO Digital Atlas. British Oceanographic Data Centre, Liverpool, 2003.

Janssen, F., Schrum, C., and Backhaus, J. O.: A climatological data set of temperature and salinity for the Baltic Sea and the North Sea, Deutsche Hydrographische Zeitschrift, 51, 5–245, 1999.

Kalberg, T., Suuroja, A., Põldvere, A., and Hints, O.: Bedrock Geological Map of Estonia, Geological Survey of Estonia and Geological Society of Estonia, 2007.

Kotilainen, A. T., Saarinen, T., and Winterhalter, B.: High-resolution paleomagnetic dating of sediments deposited in the central Baltic Sea during the last 3000 years, Mar. Geol., 166, 51–64, 2000.

Lougheed, B. C., Snowball, I., Moros, M., Kabel, K., Muscheler, R., Virtasalo, J. J., and Wacker, L.: Using an independent geochronology based on palaeomagnetic secular variation (PSV) and atmospheric Pb deposition to date Baltic Sea sediments and infer 14C reservoir age, Quaternary Sci. Rev., 42, 43–58, 2012.

Mangerud, J., Bondevik, S., Gulliksen, S., Karin Hufthammer, A., and Høisæter, T.: Marine 14C reservoir ages for 19th century whales and molluscs from the North Atlantic, Quaternary Sc. Rev., 25, 3228–3245, 2006.

Matthäus, W. and Schinke, H.: The influence of river runoff on deep water conditions of the Baltic Sea, Hydrobiologia, 393, 1–10, 1999.

Meyer, M. and Harff, J.: Modelling Palaeo Coastline Changes of the Baltic Sea, J. Coast. Res., 213, 598–609, 2005.

Olsen, J., Rasmussen, P., and Heinemeier, J.: Holocene temporal and spatial variation in the radiocarbon reservoir age of three Danish fjords, Boreas, 38, 458–470, 2009.

Olsson, I.: A warning against radiocarbon dating of samples containing little carbon, Boreas, 8, 203–207, 1979.

Olsson, I.: Content of C-14 in marine mammals from northern Europe, Radiocarbon, 22, 662–675, 1980.

Paukstys, B. and Narbutas, V.: Gypsum Karst of the Baltic Republics, Gypsum karst of the World, Int. J. Speleol., 25, 279–284, 1996.

Philippsen, B. and Heinemeier, J.: Freshwater reservoir effect variability in Northern Germany, Radiocarbon, in press, 2013.

Punning, J.-M., Vaikmäe, R., and Mäekivi, S.: Oxygen-18 variations in the Baltic Sea, The International journal of radiation applications and instrumentation, Nucl. Geophys., 5, 529–539, 1991.

Reimer, P. J., Baillie, M. G. L., Bard, E., Bayliss, A., Beck, J. W., Bertrand, C. J. H., Blackwell, P. G., Buck, C. E., Burr, G. S., Cutler, K. B., Damon, P. E., Edwards, R. L., Fairbanks, R. G., Friedrich, M., Guilderson, T. P., Hogg, A. G., Hughen, K. A., Kromer, B., McCormac, G., Manning, S., Ramsey, C. B., Reimer, R. W., Remmele, S., Southon, J. R., Stuiver, M., Talamo, S., Taylor, F. W., van der Plicht, J., and Weyhenmeyer, C. E.: IntCal04 terrestrial radiocarbon age calibration, 0–26 cal kyr BP, Radiocarbon, 46, 1029–1058, 2004.

Reimer, P. J., Baillie, M. G. L., Bard, E., Bayliss, A., Beck, J. W., Blackwell, P. G., Ramsey, C. B., Buck, C. E., Burr, G. S., Edwards, R. L., Friedrich, M., Grootes, P. M., Guilderson, T. P., Hajdas, I., Heaton, T. J., Hogg, A. G., Hughen, K. A., Kaiser, K. F., Kromer, B., McCormac, F. G., Manning, S. W., Reimer, R. W., Richards, D. A., Southon, J. R., Talamo, S., Turney, C. S. M., van der Plicht, J., and Weyhenmeyer, C. E.: IntCal09 and Marine09 Radiocarbon Age Calibration Curves, 0–50,000 Years cal BP, Radiocarbon, 51, 1111–1150, 2009.

Reinholdsson, M., Snowball, I., Zillén, L., Lenz, C., and Conley, D. J.: Magnetic enhancement of Baltic Sea sapropels by greigite magnetofossils, Earth Planet. Sc. Lett., 366, 137–150, 2013.

Rößler, D., Moros, M., and Lemke, W.: The Littorina transgression in the southwestern Baltic Sea: new insights based on proxy methods and radiocarbon dating of sediment cores, Boreas, 40, 231–241, 2011.

Ruff, M., Szidat, S., Gäggeler, H. W., Suter, M., Synal, H.-A., and Wacker, L.: Gaseous radiocarbon measurements of small samples, Nucl. Instrum. Methods B, 268, 790–794, 2010.

Siegenthaler, U. and Oeschger, H.: Prediction of future CO2 concentrations in the atmosphere, Cell. Mol. Life Sci., 36, 783–786, 1980.

Siegenthaler, U., Heimann, M., and Oeschger, H.: 14C Variations Caused by Changes in the Global Carbon Cycle, Radiocarbon, 22, 177–191, 1980.

Sohlenius, G., Sternbeck, J., Andrén, E., and Westman, P.: Holocene history of the Baltic Sea as recorded in a sediment core from the Gotland Deep, Mar. Geol., 134, 183–201, 1996.

Stephens, M. B., Wahlgren, C.-H., and Weihed, P.: Tektoniska enheter in den svenska berggrunden, Swedish Geological Survey (SGU), Uppsala, 1994.

Stuiver, M., Reimer, P. J., Bard, E., Beck, J. W., Burr, G. S., Hughen, K. A., Kromer, B., McCormac, G., van der Plicht, J., and Spurk, M.: INTCAL98 radiocarbon age calibration, 24,000–0 cal BP, Radiocarbon, 40, 1041–1083, 1998.

Tanaka, N., Monaghan, M. C., and Rye, D. M.: Contribution of metabolic carbon to mollusc and barnacle shell carbonate, Nature, 320, 520–523, 1986.

Wacker, L., Lippold, J., Molnár, M. and Schulz, H.: Towards radiocarbon dating of single foraminifera with a gas ion source, Nucl. Instrum. Meth. B, 294, 307–310, 2013.

Widerlund, A. and Andersson, P. S.: Late Holocene freshening of the Baltic Sea derived from high-resolution strontium isotope analyses of mollusk shells, Geology, 39, 187–190, 2011.

Willumsen, P. S., Filipsson, H. L., Reinholdsson, M., and Lenz, C.: Surface salinity and nutrient variations during the Littorina Stage in the Fårö Deep, Baltic Sea, Boreas, 42, 210–223, 2013.

Zillén, L., Conley, D. J., Andrén, T., Andrén, E., and Björck, S.: Past occurrences of hypoxia in the Baltic Sea and the role of climate variability, environmental change and human impact, Earth-Sci. Rev., 91, 77–92, 2008.